Synthesis And Characterization Of Polypyrrole-Zinc Oxide Core-Shell Hybrid Polymer Nanocomposites

Dr.N.Dhachanamoorthi, Dr.M.Jothi, S.Tamilselvan,

Abstract: Synthesis of hybrid functional nanocomposites (PPy-ZnO) was employed with ZnO by mechanical mixing method, this system, the observed FT-IR results ensured the presence of PPy in the composite and also pronounces the characteristic absorption peaks of ZnO around 591 and 438 cm−1. The observed strong vibration in the low wave number region around 591cm−1 is corresponds to antisymmetric vibrations of Zn-O-Zn bond of Zinc oxide. This ensured the presence of ZnO incorporated in the PPy nanoparticles. UV-Vis absorption spectra of PPy-ZnO nanocomposites helps to explore the optical behavior of incorporated nanoparticles into PPy matrix and hence, the integrated ZnO nanoparticles gives rise to the red shift of π–π* transition of polypyrrole. The XRD pattern exhibits the crystalline nature of PPy-ZnO nanocomposite and reveal out the existence of different crystallite sizes observed from diffraction peaks. Thermal stability of both polypyrrole and PPy-ZnO nanocomposite was investigated by thermo gravimetric analysis (TGA) and Differential scanning calorimetry (DSC). SEM images reveal that ZnO nanoparticles is deposited on the PPy surface which have a nucleus effect on the polymerization of PPy. It also ensures, the degree of deposition on the surface of PPy increases with ZnO content. SEM images indicated that the zinc particles are embedded in the PPy matrix forming the core-shell structure. ZnO nanoparticles exist as agglomerates due to high surface area and magneto dipole-dipole interactions between the particles. In SEM images, the black core is zinc particles with the diameter range of 50-150 nm and the light colored shell is attributed to PPy in the nanocomposites, which is due to the different electron penetrability. The EDAX results of PPy-ZnO reveals that an elements like Carbon (44.23 wt.%) and Sulfur (3.18 wt.%) molecules decreases and Zinc (23.47 wt.%), Oxygen(29.12 wt.%) molecules increases, while increasing concentration of ZnO nano metal oxide content.

Index Terms: Conducting Polymer, Polypyrrole, Polypyrrole-ZnO nanocomposite, Nanoparticles.

1. INTRODUCTION

Hybrid nanocomposites materials are one of the most rapidly expanding areas in material physics and chemistry. Many polymers nanocomposite materials have been developed using mechanical mixing. These materials can be prepared as both crystalline and amorphous materials. These materials have been found to have better properties than the simple salts of the metals as they show good selectivity towards some particular metal ions [1]. The hybrid polymer nanocomposites (HPnCs) have attracted considerable academic and scientific interest because of their potential applications in a variety of areas, such as drug deliveries, chemical-biosensors, encapsulation, nanoscale electronics, optoelectronics, and electrochemical and electromechanical devices. Hybrid polymer nanocomposites (HPnCs) are novel types of materials that are composed of two or more phases of different chemical constituents or structure, and at least one the chemical and structural phases is in nanometric dimension [2]. In recent years, the interest in the development of hybrid polymer nanocomposites (HPnCs) has grown rapidly due to a wide range of the potential use of these materials. Along with these materials, one significant class is that, in which the organic part is conducting polymers, such as polyaniline (PANI), polythiophene (PThi) or polypyrrole (PPy).

- *Dr.N Dhachanamoorthi, Assistant Professor & Head, PG Department of Physics, Vellalar College for Women, Erode, Tamilnadu, India .PH-+918778134822 E-mail: dhachu83@gmail.com*
- *Dr.M.Jothi, Assistant Professor, PG Department of Physics, Vellalar College for Women, Erode, Tamilnadu, India .PH-+919655669858. E-mail: jothibalajee@gmail.com*
- *S.Tamilselvan, Assistant Professor of Physics, Nandha Arts and Science College, Erode, Tamilnadu, India PH-+919994206587. E-mail: tamilpriyan001@gmail.com*

unique properties with high electrical conductivity, relatively good environmental stability, nontoxicity, relatively low cost and ease of preparation which are favorable for various types of applications. The mentioned merits lead polypyrrole to have wide potential applications in various fields, such as sensors, actuators and electric devices. On the other hand, the metal oxide nanoparticles have attracted much attention in recent years due to their interesting properties and potential applications in technological fields [3]. Zinc oxide nanoparticles (nZnO) have applications in catalysis, conductive inks, thick film pastes and adhesives for various electronic components, in photonics and in photography. Therefore, the preparation of hybrid polymer nanocomposites (HPnCs) becomes a novel challenge for the researchers. However, HPnCs are easy to prepare in nature and generally soluble in common solvents, so it is easy to prepare homogeneous and stable hybrid HPnCs by conventional blending or mixing in solution or melt form. However, the above HPnCs have an intrinsic tendency to agglomerate due to their increased electrostatic and van der Waals interactions arising from the increased surface areas. It has thus been of both theoretical and practical importance and concern to prepare unagglomerated nanocomposites with controlled distribution, shape and sizes. Many chemical methods have been developed for the incorporation of metal oxide nanoparticles into conducting polymers [1]. Herein, reported a simple synthesis of PPy-ZnO hybrid nanocomposites by mechanical mixing method, it was found that the HPnCs possessed enhanced structural, optical, crystalline nature, thermal, surface morphology and thermal properties were studied. Schematic diagram of formation mechanism of PPy-ZnO hybrid nanocomposite is as shown in Fig.5.1. The synthesized PPy-ZnO hybrid nanocomposite were characterized by Fourier transform infrared (FTIR), Ultraviolet-Visible spectroscopy (UV–vis), X-ray diffraction (XRD), Thermo gravimetric analysis (TGA), Differential scanning calorimetry (DSC), Scanning Electron Microscopy (SEM), and Energy dispersive X-ray analysis spectroscopy (EDAX).

2 EXPERIMENTAL

2.1. Materials

All of the chemical reagents used in this experiment were A.R. grade. The monomer pyrrole (PPy) and Dodecylbenzene Sulfonic acid (DBSNa) as dopant was purchased from Aldrich Chemical and purified by distillation under reduced pressure, stored in refrigerator before use. zinc oxide nanoparticles, <100 nm (98% purity) from Aldrich Chemical, Ammonium peroxydisulfate (99%, Merck), Ethonal (99% purity, Merck), Acetone (99% purity, Merck) were purchased from Merck chemical. The water used throughout the work is distilled water.

2.2. The Preparation of Polypyrrole (PPy)

The polypyrrole was synthesized by chemical oxidation polymerization under static condition in a lower temperature. About 900 ml of de ionized water was taken in a flask and an arrangement for mechanical stirring. Dodecylbenzene sulfonic acid solution (DBSNa) as a dopant was dissolved in above 900 ml of deionized water and the solution was well stirred in the flask. Monomer pyrrole was added in the above suspension solution and keeps stirring for 30min. After 30 minammonium peroxydisulfate (NH4)2S2O8 as an oxidant was added drop wise slowly to the good degree of polymerization is achieved the suspension solution was dark black in color. The entire solution mixture was continuously stirred well at 0-5◦C and the reaction was continued for another 24 h over all time speed of rotation maintained at 700rpm. The product was filtered and washed with deionized water, ethanol and acetone, then dried under vacuum at 80◦C for 24 h. Experimental setup as shown in Fig.1.

2.3. Synthesis of Polypyrrole-Zno Nanocomposites

PPy-ZnO nanocomposites were synthesized using different wt% of ZnO with respect to polypyrrole which are referred as PPy-ZnO nanocomposites. Pure PPy was synthesized following the same procedure without ZnO nanoparticles. The molar ratio of polymer (PPy) and metal Oxide ZnO was 1:0.25 to prepare PPy-ZnO (25%) nanocomposites by using mechanical mixing method. Similarly the samples were prepared in the different weight % of ZnO nanoparticles like PPy-ZnO (50%) and PPy-ZnO (100%) by the ratio 1:0.50 and 1:1 respectively.

3. RESULT AND DISCUSSION

3.1. FTIR SPECTRAL ANALYSIS

Fig.1 shows the FTIR spectrum of pure PPy, PPy-ZnO (25-100%) nanocomposites and pure zinc oxide nPs. For pure PPy, the peaks appeared at 3492.24 cm−1 corresponds to the N-H stretching vibrations. The peaks appeared around 1532.57 cm−1 could be assigned to C=C stretching vibration and the peak appeared at 1189 cm−1 was related to C-N stretching wagging vibration. The vibrations at 1115.44 cm−1 belonged to the in-plane bending vibrations of C-H. The broad band from 1000 to 900 cm−1 is attributed to C–H out-plane bending vibrations [4]. The strong vibration around 491cm−1 is observed in PPy-ZnO nanocomposites, in the low wave number region, which corresponds to antisymmetric Zn-O-Zn mode of the zinc oxide. The above results indicate the presence of PPy in the hybrid nanocomposites and also the appearance of the characteristic absorption bands for ZnO at around 491 cm−1. This suggests the presence of ZnO inside the PPy chain. However, the characteristic peaks of ZnO (491 cm−1) can be observed in Fig.1 and shifted to lower wavenumbers (498cm−1). These results reveal the interaction between ZnO nPs and PPy chain to obtain the PPy-ZnO nanocomposites [5]. The FTIR spectrum of PPy-ZnO hybrid nanocomposites is almost identical to that of pure PPy. PPy-ZnO hybrid nanocomposites show some shift in the wavenumber as well as in the intensity of peaks as compared to pure PPy. These shifts increase with the amount of metal oxide nanoparticles and could be due to the interaction between the conjugated macromolecular chain and the oxide via H-bonding between the PPy rings and the oxide particles or via interactions between the nitrogen atoms of PPy and Zn. Such interactions have also been confirmed by thermogravimetric analysis [2]. So the introduction of Zn does not damage the backbone structure of PPy and there are some interactions between them. Furthermore, a strong peak may originate from the absorption assignable to doped PPy or the interactions at the interface of ZnO nPs and PPy. Interestingly, the peaks in the nanocomposites was much stronger than that in pure PPy, which could be attributed to the amplified contribution of the charge-transfer effect between the polymer chains of PPy and ZnO nPs. It is suggested that the doped ions in the conductive PPy may bring an alteration of the local Fermi level of the Zn nanoparticles and the energy levels in the PPy molecules, thus achieve an optimal energy matching [1]. These results prove that the structure of PPy backbone in PPy-ZnO hybrid nanocomposites is similar to that of conventional PPy synthesized by the this method, The FTIR spectroscopy analysis of pure PPy, PPy-ZnO (25-100%) nanocomposites and pure ZnO nPs are shown in Table.1.

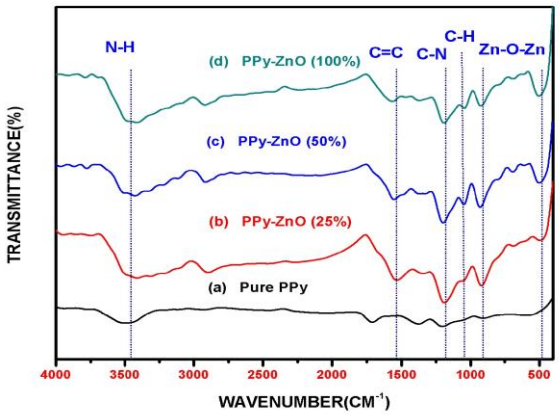

Fig.1 *FTIR spectra of pure PPy (a) and PPy-ZnO nanocomposites (b, c & d)*

Sample Name	N-H stretching vibrations (cm-1)	C=C ring symmetric stretching vibrations (cm-1)	C-N stretching wagging vibrations (cm-1)	In-plane C–H bending Vibrations (cm-1)	Out-plane C–H bending Vibrations (cm-1)
Pure PPy	3492.24	1532.57	1189.72	1115.44	906.34
PPy-ZnO (25%)	3410.76	1546.41	1180.62	1110.50	917.58
PPy-ZnO (50%)	3419.85	1564.19	1175.05	1110.31	921.28
PPy-ZnO (100%)	3410.78	1533.71	1170.81	1108.30	921.07

Sample Name	Wavelength (nm)			Absorption			Band gap (eV)
	Band: 1	Band: 2	Band: 3	Band: 1	Band: 2	Band: 3	
Pure PPy	260	473	931	0.1826	0.1581	0.2017	3.46
PPy-ZnO (25%)	495	695	960	0.4001	0.3592	0.4069	2.74
PPy-ZnO (50%)	588	783	1031	0.2458	0.2909	0.3724	2.55
PPy-ZnO (100%)	586	871	1070	0.1003	0.1274	0.1707	3.15
Pure ZnO	582	870	1070	0.1001	0.1100	0.1245	1.18

Table.1 *FTIR data of pure PPy and PPy-ZnO Nanocomposites*

3.2. UV-VIS ABSORPTION SPECTRAL ANALYSIS

The UV-vis absorption spectrum of pure PPy, PPy-ZnO (25-100%) nanocomposites, pure ZnO nPs dispersed in aqueous medium is shown in Fig.2. The spectra of pure PPy shows, three characteristic absorption peaks appeared in which the first appeared at 260 nm can be ascribed to π-π* transition of the benzenoid rings, while the other peaks appeared at 473 and 931 nm can be attributed to polaron-π* transition and π-polaron transition respectively, Furthermore the peaks appeared at 473 and 931 nm are related the formation of polaron which proves that pyrrole molecules have been polymerized into PPy [3]. The absorption band observed at 473 nm and 931 nm for π-π* transition can also be attributed to the electronic transitions between quinoid and benzenoid structures of PPy. Polymer nanocomposites (25-100%) have three characteristic absorption peaks obtained, when the peaks of PPy-ZnO nanocomposites are compared with pure PPy, one can inferred that the intensity of peaks decreased with increasing the metal oxide concentration (from 25% to 100%) were shown in Fig.2 The optical band gap in a polymer nanocomposites is determined by plotting absorption coefficients (α) as (αhv)m vs hv where 'm' represents the nature of the transition and hv is the photon energy. Now 'm' may have different values, such as $\frac{1}{2}$, 2, $\frac{3}{2}$ and 3 for allowed direct, allowed indirect, forbidden direct and forbidden indirect transitions respectively. The optical absorption coefficient (α) near the absorption edge for direct interband transitions is given by the equation (1).

$$\alpha = \frac{A(h\nu - E_g)^{\frac{1}{2}}}{h\nu} \quad (1)$$

Where, A is the absorption constant for a direct transition. For allowed direct transition one can plot (αhv)2 vs. hv as shown in Fig.3a-3e and extrapolate the linear portion of it to α=0 value to obtain the corresponding band gap [6]. UV-vis spectral and band gap data of PPy, PPy-ZnO nanocomposites (25-100%) and pure ZnO nPs is shown in Table.2.

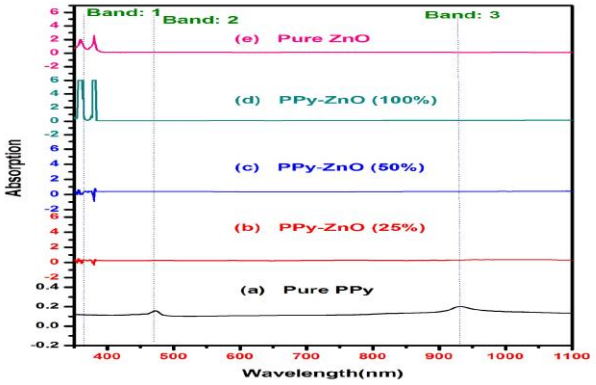

Fig.2 *UV-vis spectra of pure PPy (a), PPy-ZnO nanocomposites (b, c, d) and pure ZnO nPs (e)*

Table.2 UV-vis spectral data of pure PPy, PPy-ZnO nanocomposites and pure ZnO nPs

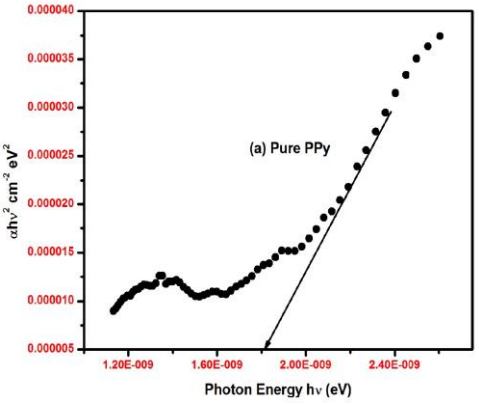

Fig: 3a

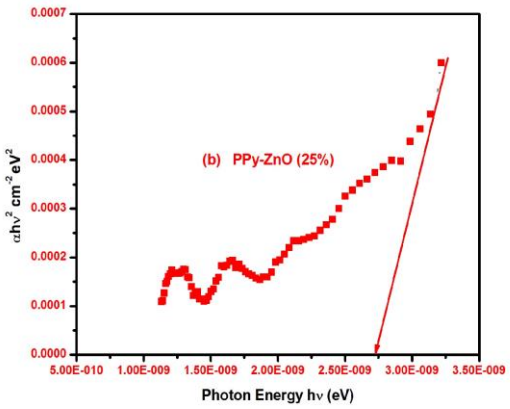

Fig: 3b

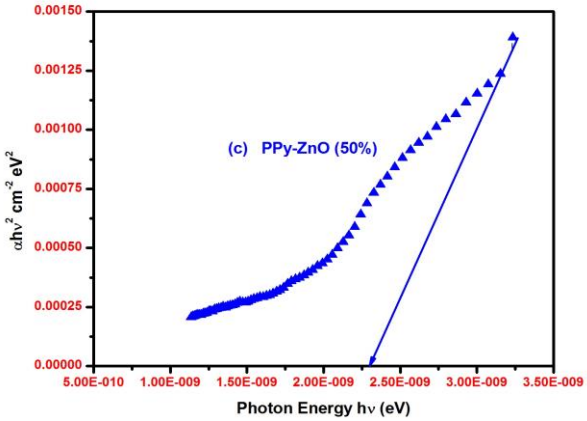

Fig: 3c

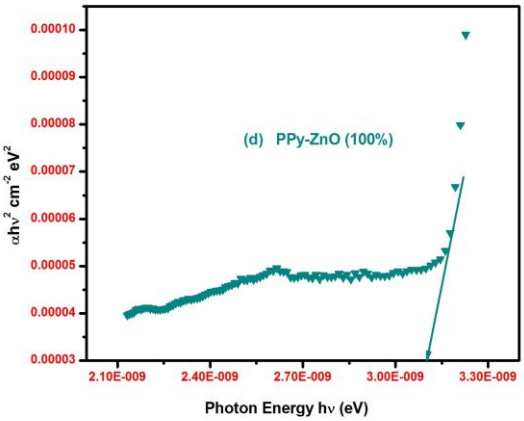

Fig: 3d

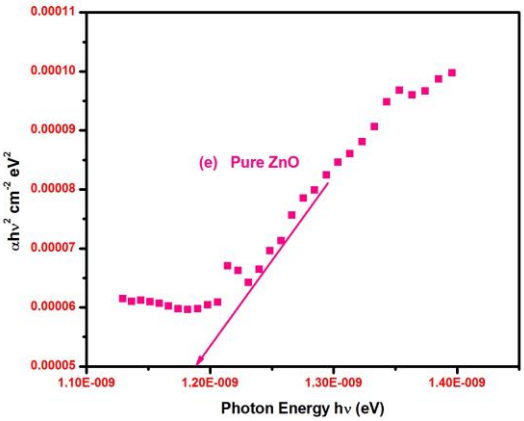

Fig: 3e

Fig.3a-3e Tauc plot for (αhν) 2 vs hν of pure PPy, PPy-ZnO nanocomposites and pure ZnO nPs

3.3. X-RAY DIFFRACTION STUDIES

X-ray diffraction (XRD) is another important tool to estimate the degree of the relative peak intensity and crystallographic parameters of the sample presented in Fig.4. Crystallite sizes were calculated from the diffraction line using Scherrer's equation, $L=k\lambda/\beta\cos\theta$, where L is the mean dimension of the crystallites, β is the full width and half maximum of the diffraction peak, θ is the diffraction angle, λ is the wavelength of the CuKα radiation (0.1540 nm), and K is equal to 0.89. Phase investigation of the crystallized products is also performed by XRD and the diffraction pattern is presented. For the pure PPy, the broad peak at 20.02° is related to the amorphous nature and the other peak appear at 44.38°, and the average crystalline size of pure PPy is 102 nm. The result supports the fact that, there is good obvious chemical interaction between PPy and ZnO in the nanocomposites. In nanocomposites samples have totally eight XRD pattern and sharp peaks was appeared and compared to pure PPy samples. XRD pattern was entirely different and almost identical only in pure ZnO nanocomposites [7]. For the nanocomposites materials with varying concentration from 25% to 100% ZnO nPs eight diffraction peaks at different 2θ positions were observed. The positions of the eight peaks vary slightly with ZnO nPs concentration as shown in Fig.4.

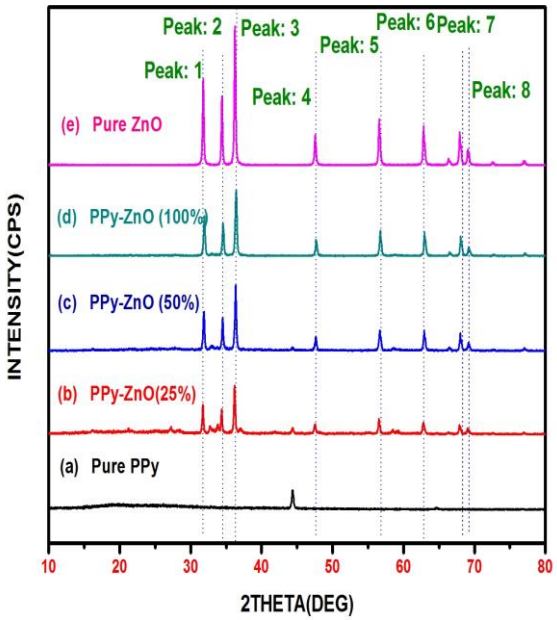

Fig.4 X-Ray diffraction patterns of pure PPy (a), PPy-ZnO nanocomposites (b, c, d) and pure ZnO nPs (e)

Peak No	Pure PPy					
	2θ	FWHM	Intensity	d Spacing Value	Crystalline size (nm)	Strain
1	20.02	0.094	243	4.4315	85	0.0010
2	44.38	0.071	840	2.0395	120	0.0003
Peak No	PPy-ZnO (25%)					
	2θ	FWHM	Intensity	d Spacing Value	Crystalline size (nm)	Strain
1	31.72	0.041	1253	2.8186	58	0.0002
2	34.40	0.141	1077	2.6049	58	0.0008
3	36.20	0.188	1987	2.4794	44	0.0011
4	47.54	0.181	390	1.9111	47	0.0007
5	56.56	0.071	673	1.6258	127	0.0002
6	62.80	0.165	500	1.4784	56	0.0005
7	67.88	0.141	403	1.3796	67	0.0004
8	69.02	0.071	273	1.3596	135	0.0002
Peak No	PPy-ZnO (50%)					
	2θ	FWHM	Intensity	d Spacing Value	Crystalline size (nm)	Strain
1	31.86	0.165	1607	2.8065	50	0.0011
2	34.54	0.141	1407	2.5946	58	0.0008
3	36.36	0.141	2770	2.4688	59	0.0008
4	47.64	0.141	613	1.9073	61	0.0006
5	56.66	0.141	880	1.6232	64	0.0005
6	62.94	0.071	873	1.4755	131	0.0002
7	68.04	0.094	687	1.3768	101	0.0002
8	69.18	0.071	283	1.3568	135	0.0001
Peak No	PPy-ZnO (100%)					
	2θ	FWHM	Intensity	d Spacing Value	Crystalline size (nm)	Strain
1	31.94	0.212	1687	2.7997	38	0.0014
2	34.58	0.212	1393	2.5917	39	0.0013
3	36.42	0.235	2743	2.4649	35	0.0013
4	47.66	0.071	703	1.9065	122	0.0003
5	56.74	0.118	1020	1.6211	76	0.0004
6	62.98	0.094	867	1.4746	99	0.0002
7	66.54	0.071	120	1.4041	133	0.0002
8	68.54	0.071	77	1.3679	135	0.0002
Peak No	Pure ZnO					
	2θ	FWHM	Intensity	d Spacing Value	Crystalline size (nm)	Strain
1	31.78	0.165	3610	2.8134	50	0.0011
2	34.44	0.141	2907	2.6019	58	0.0008
3	36.26	0.141	5833	2.4754	59	0.0008
4	47.54	0.118	1173	2.9111	73	0.0005
5	56.60	0.141	1933	1.6248	63	0.0005
6	62.86	0.071	1660	1.4772	131	0.0002
7	67.94	0.188	1397	1.3786	50	0.0005
8	69.06	0.118	663	1.3589	81	0.0003

Table .3 *X-Ray diffraction patterns of pure PPy (a), PPy-ZnO nanocomposites (b, c, d) and pure ZnO nPs (e)*

The average crystallite size was calculated for pure PPy, PPy-ZnO (25-100%) and pure ZnO nPs are reported (PPy-ZnO: 25%-74 nm; PPy-ZnO: 50%-82 nm; PPy-ZnO: 100%-84 nm). The smallest crystallite size (70 nm) was observed for pure PPy. The above results indicate the average crystallite size (70 nm) is increased with increasing Zn ion concentration. Strain and dislocation density also calculated for pure PPy and PPy-ZnO nanocomposites samples as shown in Table.3. However, after a combination with PPy, the peak intensity of hybrid PPy-ZnO nanocomposites increased due to the amorphous PPy layers with increasing the dopant percentage of zinc oxide [8]. The intensity of characteristics diffractions peaks of PPy in the nanocomposites is increasing ZnO content which reveals that ZnO nanoparticles have influenced the crystalinity of PPy. Thus, XRD results indicate that there is change in the crystalline structure of the nanocomposite after Zn adsorption. Crystallite size and crystalline properties of PPy-ZnO (25-100%) hybrid nanocomposites and pure ZnO is shown in Table.3.

3.4. Thermogravimetric Analysis

Thermal gravimetric analysis was performed in order to investigate the thermal stability of the nanocomposite and the resultant thermogram is discussed. The thermal decomposition curves of pure PPy, PPy-ZnO (25-100%) nanocomposites and pure ZnO nPs under N2 atmosphere are shown in Fig.5. The samples were heated from 0 to 500 ºC at a rate of 10.0 (K min-1). For pure PPy, the initial weight loss (-32.28%) occurred below (100 ºC) and is attributed to the evaporation of moisture and loss of some impurities via degradation. Subsequently, successive degradation from 200 ºC corresponds to polymer decomposition [6]. The thermogram of pure PPy has four-step weight loss. The first initial weight loss is due to the removal of adsorbed moisture. The second weight loss can be attributed to loss volatile material. The third one was ascribed to the elimination of dopants. Finally fourth step shows a massive weight loss, that it is owing to the degradation of the polymer chain. The residual mass and residual temps of pure PPy were 28.77 ºC and 497.9 ºC respectively. The thermogravimetric study of PPy-ZnO nanocomposites shows single step decomposition following on the small initial weight loss due to the removal of moisture. In case of PPy-ZnO nanocomposites, three steps weight loss can be seen. The first and second steps of weight loss were observed in polypyrrole thermogram due to the removal of moisture and volatile materials. The third step weight loss which is attributed to polymer chain decomposition begins in temperature higher than that of ZnO thermal degradation [3,9]. By comparing the thermograms of synthesized pure PPy and PPy-ZnO nanocomposites one can be understand that main effect of ZnO is greatly improved in thermal stability of nanocomposites from 25% to 100%. When PPy-ZnO (25%) nanocomposite samples compared with the pure PPy, the weight loss decreased with increasing the ZnO weight concentration, the residual mass and temperature of the PPy-ZnO (25%) was 64.91% and 497.7 ºC respectively. The pure ZnO shows almost very small weight change in the whole temperature range. In comparison, the pure PPy and nanocomposite PPy-ZnO (25-100%) samples and pure ZnO, the mass change, residual mass, were decreased with increasing then ZnO weight concentration by residual temperature maintain as constant value. From these results, it is found that the thermal stability of the nanocomposite could be improved with an increase in the ZnO content.

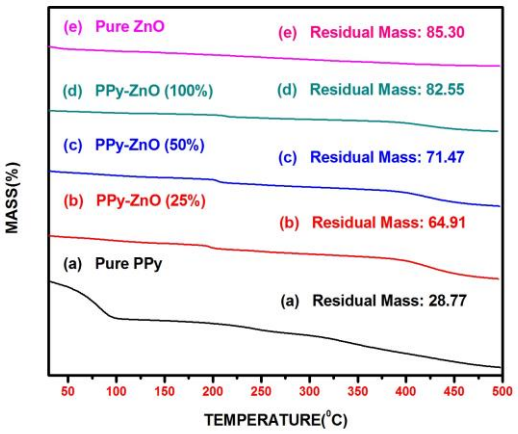

Fig.5 *TGA spectra of pure PPy (a), PPy-ZnO Nanocomposites (b, c, d) and pure ZnO nPs (e)*

Pure PPy			
Mass Change	Mass	Residual Mass	Residual Temp
Stage: 1	-32.28	28.77	497.90
Stage: 2	-5.79		
Stage: 3	-7.11		
Stage: 4	-12.83		
Stage: 5	-		
PPy-ZnO (25%)			
Mass Change	Mass	Residual Mass	Residual Temp
Stage: 1	-3.42	64.91	497.70
Stage: 2	-2.99		
Stage: 3	-5.45		
Stage: 4	-7.15		
Stage: 5	-16.08		
PPy-ZnO (50%)			
Mass Change	Mass	Residual Mass	Residual Temp
Stage: 1	-2.75	71.47	497.70
Stage: 2	-3.96		
Stage: 3	-3.30		
Stage: 4	-5.72		
Stage: 5	-12.8		
PPy-ZnO (100%)			
Mass Change	Mass	Residual Mass	Residual Temp
Stage: 1	-2.61	82.55	497.70
Stage: 2	-3.39		
Stage: 3	-3.17		
Stage: 4	-8.28		
Stage: 5	-		
Pure ZnO			
Mass Change	Mass	Residual Mass	Residual Temp

Stage: 1	-7.05		
Stage: 2	-7.65		
Stage: 3	-	85.30	497.80
Stage: 4	-		
Stage: 5	-		

Fig.5 *TGA spectra of pure PPy (a), PPy-ZnO Nanocomposites (b, c, d) and pure ZnO nPs (e)*

3.5. Differential Scanning Calorimetric Analysis

Differential scanning calorimetric spectra were recorded for the pure PPy, PPy-ZnO (25-100%) nanocomposites and pure ZnO nPs and shown in Fig.6a-6e. The figure shows a broad endothermic perk centered on at 340.2 ºC. This indicating the elimination of physically attached water molecules from the surface of the compound. Additionally several sharp exothermic peaks were appeared at about 86.7 ºC, which was the complex peak and the area of this peak is 483.7J/g. The onset and endset temperature of the complex peak are 58.6 ºC and 106.2 ºC respectively, which is presumably due to the polymer decomposition. The DSC spectrum of PPy-ZnO (25-100%) and pure ZnO are shown in Fig.6a-6e. The peaks were indicating that the polymer decomposition was takes place in PPy-ZnO nanocomposites but it is clearly absent in ZnO nPs. Despite the degradation of PPy-ZnO (25-100%), samples indicating the gradual enhancement of thermal stability of the polymer chain with increasing the amount of ZnO [9-11]. The exothermic peak disappeared for pure ZnO samples, indicating strong interaction of the oxide with the polymer chain.

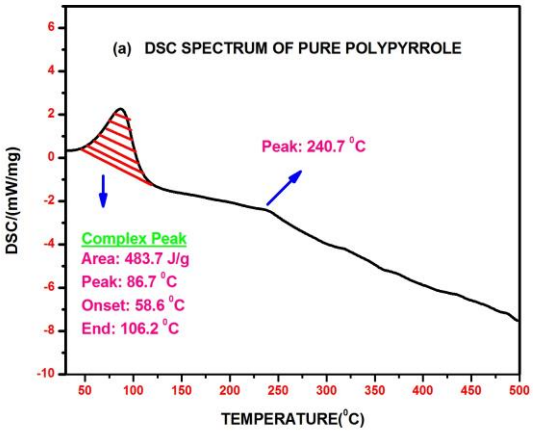

Fig: 6a

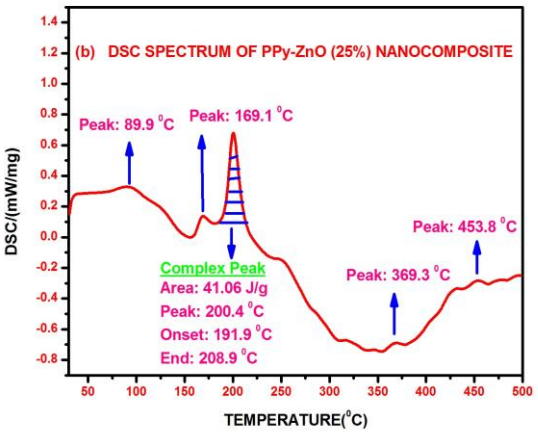

Fig: 6b

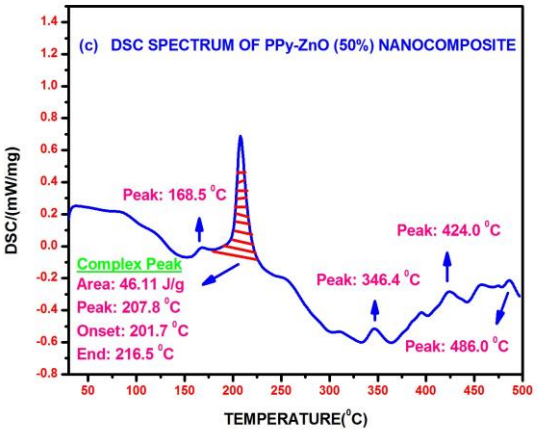

Fig: 6c

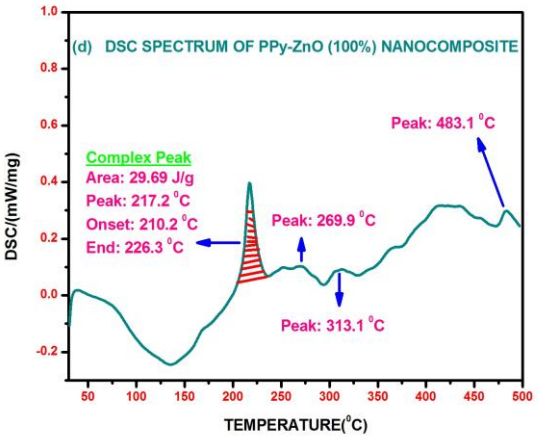

Fig: 6d

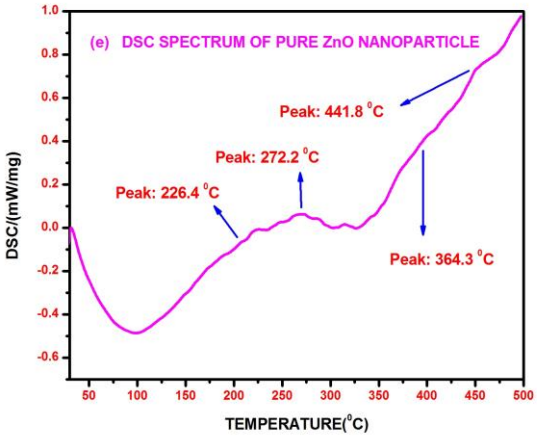

Fig: 6e

Fig.6a-*6e DSC spectra of pure PPy (a), PPy-ZnO nanocomposites (b, c,d), pure ZnO nPs (e)*

4.6. SCANNING ELECTRON MICROSCOPIC STUDIES

SEM morphology of pure PPy, PPy-ZnO (25-100%) nanocomposites and pure ZnO nanoparticles are shown in Fig.7 (a-e). From the Fig.7a, SEM image of pure PPy which suggests that the particle exhibits a spherical in nature. The micrographs of PPy-ZnO (25-100%) nanocomposites are shown in Fig.7 (b-d). SEM images of PPy-ZnO (25-100%) nanocomposites reveal that PPy is deposited on the surface of ZnO nPs, which have a nucleus effect on the polymerization of PPy [12]. The observed SEM images show that the surface morphologies of PPy-ZnO (25-100%) nanocomposites are strongly affected by the ZnO content. SEM micrograph concludes the formation of PPy-ZnO nanocomposites on lattices that are fibril in nature. SEM images indicate that the Zn particles are embedded in the PPy matrix forming the core-shell structure [12,13]. ZnO nanoparticles exist as agglomerates are due to high surface area and magneto dipole-dipole interactions between the particles. The dark core is ZnO nPs and the light colored shell is PPy in the nanocomposites, which is due to the different electron penetrability [14]. Therefore, ZnO as an anchor agent played an important role. The amphiphilic ZnO would be beneficial for the adherence between the polymer shell and the inorganic core. The adsorbed ZnO might provide active sites on the zinc particles, so as to induce the growing polycationic PPy chains to complete the coating of PPy layers, leading to the formation of PPy-ZnO nanocomposites [15]. It indicates that the nanocomposites are composed of crystalline zinc particles and polycrystalline PPy, which is in accordance with the results obtained by XRD analysis.

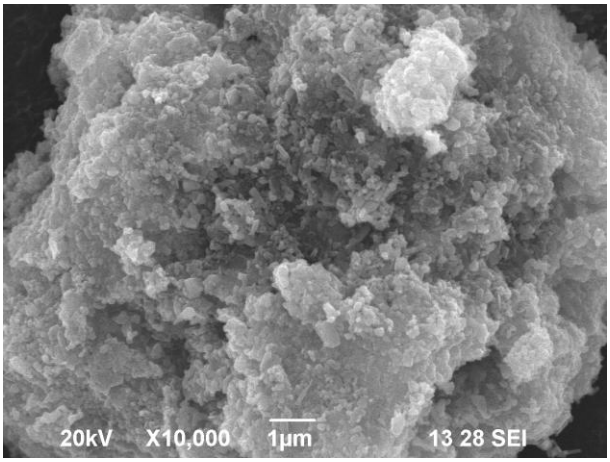

Fig: 7a

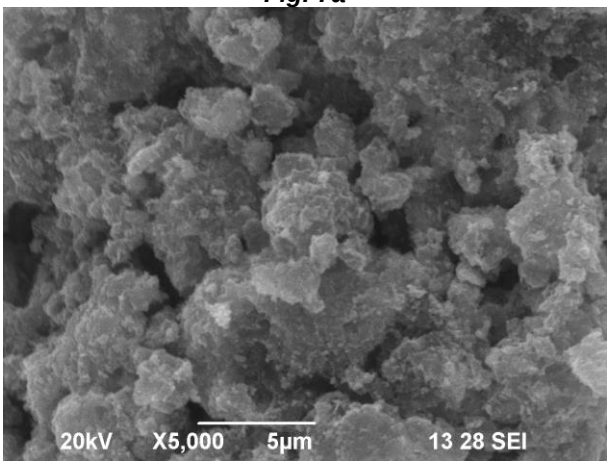

Fig: 7b

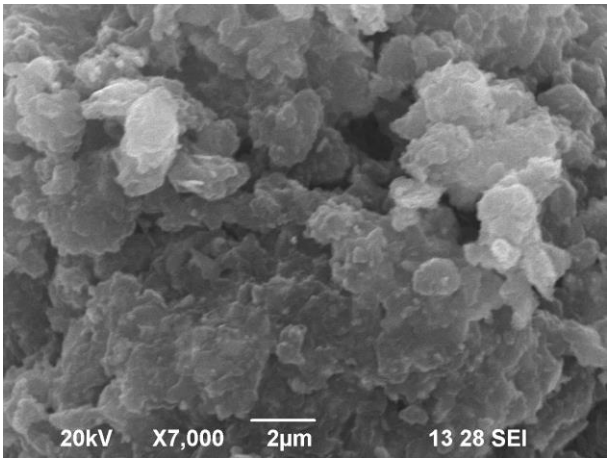

Fig: 7c

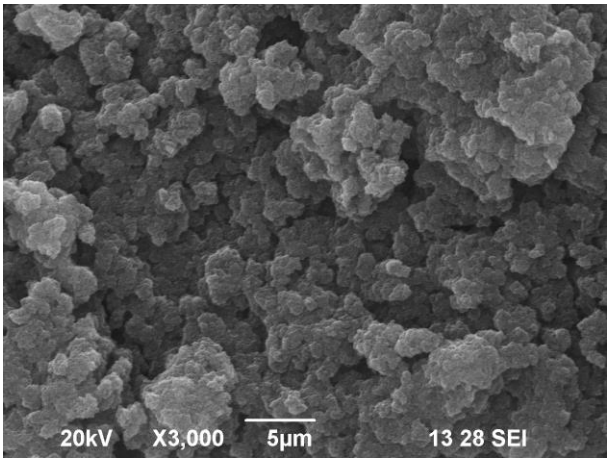

Fig: 7d

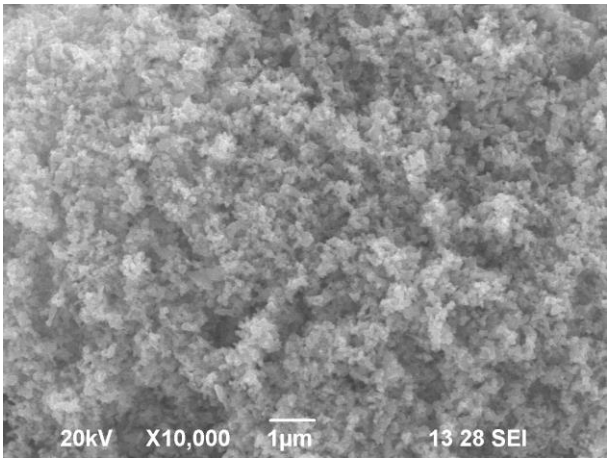

Fig: 7e

Fig.7a*-7e SEM images of pure PPy (a), PPy-ZnO nanocomposites (b, c, d), pure ZnO nPs (e)*

4.7. ENERGY DISPERSIVE X-RAY ANALYSIS

Energy dispersive X-ray analysis (EDAX) was used to analyze the elemental constituents of the pure PPy, PPy-ZnO (25-100%) nanocomposites and pure ZnO nPs the corresponding element contents are listed in Table.5. Fig.8a illustrates the atomic weight (%) of carbon, oxygen and sulfur was 72.06%, 22.17% and 5.77% respectively. As shown in the Table.5, atomic weight of carbon is decreased with increasing the concentration of ZnO. In case of PPy-ZnO nanocomposites (25-100%) the carbon and sulfur content was decreased, while the oxygen and zinc contents were increased with increasing concentration of ZnO nPs in the composites [16,17]. It turns out that the zinc oxide concentration plays an important role that increasing the concentration of zinc oxide with PPy nanocomposites are formed and started to cover the entire surface of PPy.

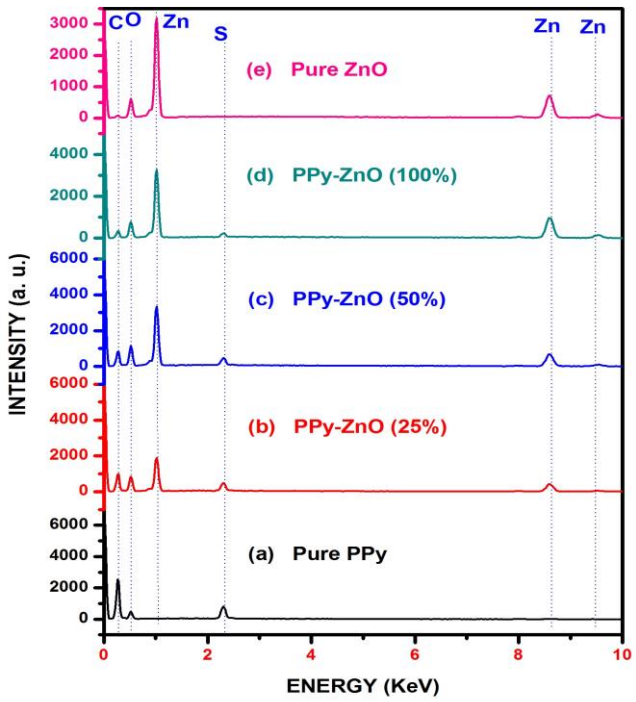

Fig.8 *EDAX spectra of pure PPy (a), PPy-ZnO nanocomposites (b,c,d) and pure ZnO nPs (e)*

Sample Name	Weight (%)				
	Carbon	Oxygen	Sulfur	Zinc	Total
Pure PPy	72.06	22.17	5.77	-	100
PPy-ZnO (25%)	44.23	29.11	3.18	23.47	100
PPy-ZnO (50%)	36.26	29.26	2.66	31.95	100
PPy-ZnO (100%)	22.36	21.00	1.62	55.01	100
Pure ZnO	25.30	74.70	-	-	100

Table.5 *Element analysis data of pure PPy, PPy-ZnO nanocomposites and pure ZnO nPs*

4. CONCLUSION

FTIR characterization revealed that the characteristics bonds were appeared in the comparative spectra of pure PPy, ZnO nPs and PPy-ZnO (25-100 wt%). These results indicate that the presence of ZnO in the matrix of PPy. From the results, one can infer that there wavenumber shift is observed in the PPy-ZnO (25-100 wt%) from the pure PPy. These results elucidated the structure of backbone of PPy-ZnO and the characteristics properties of pure PPy, ZnO nPs. From the UV-visible characteristics bands one can observe that, the three absorption peaks observed which may be due to the transition of π-π* in the case of the pure PPy. From the band gap calculations, it is clearly seen that, there is a decrease from 2.74 to 2.55 eV of band gap value, when we move from PPy-

ZnO (25 wt%) to PPy-ZnO (50 wt%). This is may be due to that the accumulation of ZnO nPs in the matrix of PPy altered the band gap characteristics and after immediately, the band gap value of PPy-ZnO (100%) is decreased. This is because, the over accumulation of ZnO nPs being saturated in the matrix of PPy and thus the same defects in the arrangement of atoms are influenced which may affect the optical band gap characteristics. Among the list of values given in the report, the lowest value of band gap was observed for ZnO nPs (1.18 eV). From the XRD studies, one broad peak and a sharp peak were observed in the case of pure PPy as previous chapter. The crystalinity is improved, when we move from 25 wt% to 100 wt% in the case of PPy-ZnO nanocomposites. This is closely similar with the pattern of ZnO nPs. From the calculation crystallite size, there is a decrease in crystallite size if we move from 25 wt% to 100 wt%. This is due to the fact that, there is increase of loading amount ZnO nPs in the matrix of PPy. This proves that the ZnO nPs are intercalculated well with PPy matrix. Similarly, the strain is getting increased (from 2x10-4 to 1.4x10-3), when we move from 25 wt% to 100 wt% in the case of PPy-ZnO. This is because, the strain is increased with the loading amount of ZnO nPs in the matrix of PPy to make the ZnO loaded matrix with more strain. The dislocation density is also changing from 2.50x10-15 to 1.51x10-15 (m-2) when we move from 25 wt% to 100 wt% in the case of PPy-ZnO (100 wt%), the value of 25 wt% is again regenerating because of some structured defects or changes which may happen for PPy-ZnO (50%). From the thermogravimentric analysis, one can conclude the thermal behavior of PPy-ZnO (25-100%) and pure PPy, ZnO nPs. These results indicate that, the residual mass and residual temperatures were changing significantly. From the data, it can be seen that there is a increasing (from 64.91 to 82.57) trend in residual mass, when we move from 25 to 100 wt%. This is because of loading amount of ZnO nPs in the matrix of PPy. But the residual temperature does not changing significantly. From the differential scanning calorimetric analysis, one can conclude that there are gradual enhancements of thermal stability of PPy by the addition of ZnO from 25 to 100%. This is because of the fact that, the matrix of PPy getting strength by the accumulation of ZnO nPs. The characteristics exothermic and endothermic peaks shows the thermal behavior of pure PPy, ZnO nPs and PPy-ZnO (25-100 wt%). From the morphology investigations of pure PPy, ZnO nPs and and PPy-ZnO (25-100 wt%) nanocomposites, one can inferred that the pure PPy shows the particles are spherical in nature, while the other cases not showing the spherical particles, when we move from 25 to 100 wt%, the accumulation of ZnO nPs fully covered on the surface of PPy. This indicates that, the surface morphology of nanocomposites is differing significantly. On the other hand, the ZnO nPs photograph is showing own topography. From the studies of elemental composition, there is a definite increment of oxygen from 29.11 to 29.26 (25 to 100 wt%). This may be due to that the ZnO nPs are loading in the PPy matrix, where considerably the oxygen content is decreased for PPy-ZnO (100 wt%). This is may be due to the fact that, the fully saturated surface may accumulate nPs and the interaction with the incident radiation can have some responsibility to exhibit the compositions.

REFERENCES

[1] Xiaoming Yang, Liang Li, Songmin Shang, Guoliang Pan, Xianghua Yu, Guoping Yan. “Facial synthesis of polypyrrole-silver nanocomposites at the water-ionic liquid interface and their electrochemical properties”. Materials Letters 64 (2010) 1918-1920.

[2] Xiaoming Yang, Liang Li, Feng Yan. “Polypyrrole-silver composite nanotubes for gas sensors”. Sensors and Actuators B 145 (2010) 495-500.

[3] Shengyu Jing, Shuangxi Xing, Lianxiang Yu, Chun Zhao. “Synthesis and characterization of Ag-polypyrrole nanocomposites based on silver nanoparticles colloid”. Materials Letters 61 (2007) 4528-4530.

[4] Hamid Heydarzadeh Darzi, Saeedeh Gilani Larimi, Ghasem Najafpour Darzi. “Synthesis, characterization and physical properties of a novel xanthan gum-polypyrrole nanocomposite”. Synthetic Metals, Article in press.

[5] B. Birsoz, A. Baykal, H. Sozeri, M.S. Toprak. “Synthesis and characterization of polypyrrole-$BaFe_{12}O_{19}$ nanocomposite”. Journal of Alloys and Compounds 493 (2010) 481-485.

[6] KaiwenXue, Yang Xu, Wenbo Song. “One-step synthesis of 3D dendritic gold- polypyrrole nanocomposites via a simple self-assembly method and their electrocatalysis for H_2O_2”. Electrochimica Acta 60 (2012) 71-77.

[7] M. Mallouki, F. Tran-Van, C. Sarrazin, C. Chevrot, J.F. Fauvarque. “Electrochemical storage of polypyrrole-Fe_2O_3 nanocomposites in ionic liquids”. Electrochimica Acta 54 (2009) 2992–2997.

[8] Qilin Cheng, Ying He, Vladimir Pavlinek, Chunzhong Li, PetrSaha. “Surfactant-assisted polypyrrole-titanate composite nanofibers: Morphology, structure and electrical properties”. Synthetic Metals 158 (2008) 953–957.

[9] Lifeng Cui, JianShen, Fangyi Cheng, Zhanliang Tao, Jun Chen, “SnO_2 nanoparticles-polypyrrole nanowires composite as anode materials for rechargeable lithium-ion batteries”. Journal of Power Sources 196 (2011) 2195–2201.

[10] Wenqin Wang, Wenli Li, Ruifeng Zhang, Jianjun Wang. ”Synthesis and characterization of Ag-PPy yolk-shell nanocomposite”. Synthetic Metals 160 (2010) 2255–2259.

[11] NirmalyaBallav, MukulBiswas. “Conductive composites of polyaniline and polypyrrole with MoO_3”. Materials Letters 60 (2006) 514-517.

[12] Lijie Hong, Yang Li, Mujie Yang. “Fabrication and ammonia gas sensing of palladium-polypyrrole nanocomposite”. Sensors and Actuators B 145 (2010) 25-31.

[13] Madhumita Bhaumik, Taile Yvonne Leswifi, ArjunMaity, V.V. Srinivasu, Maurice S. Onyango. “Removal of fluoride from aqueous solution by polypyrrole-Fe_3O_4 magnetic Nanocomposite”. Journal of Hazardous Materials 186 (2011) 150-159.

[14] C.Lai, G.R. Li, Y.Y. Dou, X.P. Gao. “Mesoporous polyaniline or polypyrrole -anatase TiO_2 nanocomposite as anode materials for lithium-ion batteries”. Electro-chimica Acta 55 (2010) 4567–4572.

[15] Yu Xie, Xiaowei Hong, YunhuaGao, Mingjun Li, Jinmei Liu, Juan Wang, Jing Lu. “Synthesis and characterization of La-Nd-doped barium-ferrite-polypyrrole nano composites”. Synthetic Metals 162 (2012) 677-681.

[16] Pi-Guey Su, Lin-Nan Huang. “Humidity sensors based on TiO2 nanoparticles-polypyrrole composite thin films”. Sensors and Actuators B 123 (2007) 501-507.

[17] Madhumita Bhaumik, Arjun Maity, V.V. Srinivasu, Maurice S. Onyango. “Enhanced removal of Cr (VI) from aqueous solution using polypyrrole-Fe_3O_4 magnetic nano-

composite". Journal of Hazardous Materials 190 (2011) 381-390.